

Fajun Zhang
Bernd Stühn

Composition fluctuation and domain spacing of low molar weight PEO–PPO–PEO triblock copolymers in the melt, during crystallization and in the solid state

Received: 7 October 2005
Accepted: 21 December 2005
Published online: 1 March 2006
© Springer-Verlag 2006

Abstract We have studied a series of PEO–PPO–PEO triblock copolymers (Pluronics) in their melt and solid state mainly using static and time-resolved small-angle X-ray scattering (SAXS). In the melt state, composition fluctuations were observed. Their temperature variation was in accordance with mean-field theory. A crossover from the mean-field regime to the fluctuation regime was observed for samples with high molar mass. To check the overall conformation of molecules in the disordered state, composition fluctuations during crystallization were investigated by time-resolved SAXS. Detailed analysis on the time dependent intensity and peak position indicate that molecules remaining in the disordered state adopt a stretched overall conformation. In the solid state, crystallization of PEO blocks induced phase separation, resulting in an alternating crystalline/

amorphous lamellar structure. Samples with short PEO block formed a simple lamellar structure with extended-chain conformation. The domain spacing increased with crystallization temperature due to the swelling of the amorphous domain by uncrystallized molecules. Samples with long PEO block formed a mixed lamellar structure. Structures with once-folded and extended PEO block coexisted in a large temperature range and their relative fraction changed with crystallization temperature. This mixed structure was reduced to a simple lamellar structure with once-folded crystalline structure at low crystallization temperatures.

Keywords Crystallization · PEO–PPO–PEO triblock copolymer · Phase separation · SAXS · Time-resolved SAXS

F. Zhang · B. Stühn (✉)
Technische Universität Darmstadt,
Institut für Festkörperphysik,
64289 Darmstadt, Germany
e-mail: stuehn@fkp.physik.
tu-darmstadt.de
Tel.: +49-6151-162783
Fax: +49-6151-164883

Introduction

Poly(ethylene oxide)–poly(propylene oxide)–poly(ethylene oxide) (EPE) triblock copolymers with low molecular weight are very important commercial products known as Pluronic and Synperonic copolymers. Because of their amphiphilic properties, i.e., the hydrophilic PEO end and hydrophobic PPO middle block, these polymers are widely used in the detergent and pharmaceutical industries [1]. Stimulated by these numerous applications, the phase behavior and micellization of Pluronics in water or in organic solvent have been extensively studied and reviewed [1–10]. However, the bulk properties of this

kind of triblock copolymers in the melt and solid states are still not well-understood [11–17]. Block lengths and purities of EP copolymers prepared by anionic polymerization of propylene oxide are usually limited by a transfer reaction, which results in low molecular weight copolymer products. Thus, the phase-separated structure in PEO/PPO copolymers has not been reported until recently by Hamley et al. and Fairclough et al. [11, 12]. Using a strictly sequential anionic polymerization technique, they prepared several EP diblock copolymers with high molecular weight and narrow distribution. The order–disorder transition of these EP diblock copolymers was determined using small-angle X-ray scattering (SAXS) [11]. The Flory–Huggins

interaction parameter, χ , of this system was also determined. Furthermore, a triblock copolymer EPE with perdeuterated PPO block was studied using small-angle neutron scattering, and the temperature dependence of the Flory–Huggins parameter was determined as $\chi = 20.2/T + 0.0221$ [12]. Based on these measurements and the analysis of mean-field and fluctuation theories of block copolymers, they predicted that the Pluronic copolymers will not exhibit microphase separation even if they were pure samples [12].

Understanding of the phase behavior of block copolymers in the liquid state has been a very active field in polymer science during the last several decades [1, 18–27]. The phase behavior of block copolymers in their melt state is determined by three factors: the overall degree of polymerization, N ; their composition, given in the simple case as the volume fraction f of one of the blocks; and the segmental interaction as described by the Flory–Huggins interaction parameter χ [1]. The first two for a given copolymer are fixed, while χ is temperature-dependent. One often finds a relation $\chi = AT^{-1} + B$, where A is a positive constant. Theoretically, for a block copolymer in its disordered state, the structure factor at temperature T has been calculated by Leibler based on a Landau-type mean-field theory [18].

$$S(q)^{-1} = [F(q) - 2\chi N]/N \quad (1)$$

where the form function $F(q)$ is expressed in terms of Debye functions. The wave vector q is defined by $q = (4\pi/\lambda) \sin(\theta/2)$, where λ and θ are the wavelength and scattering angle. $S(q)$ exhibits a maximum, which decreases with increasing temperature due to the temperature dependence of χ . It is located at a scattering vector q^* , which is determined by the size of the blocks of the copolymer. The experimentally observed intensity at a given scattering vector q is directly proportional to the structure factor (Eq. 2). The contrast factor K involves instrumental parameters and the scattering contrast between both blocks of the copolymer. As a consequence of the temperature dependence of χ , the reciprocal intensity $I_{\max}^{-1}(q^*)$ varies linearly with T^{-1} (Eq. 3).

$$I(q) = K \cdot S(q) \quad (2)$$

$$I_{\max}^{-1}(q^*) \propto S^{-1}(q^*) \propto \frac{1}{T_s} - \frac{1}{T} \quad (3)$$

By extrapolating I_{\max} to infinity, the critical temperature, T_s , predicted by mean-field theory may be obtained. However, experimental results in general do not support this prediction. In many reported works, the intensity data were clearly found to deviate from the linear relationship

Eq. 3 when approaching the disorder to order transition temperature [19, 20]. Fredrickson and Helfand modified Leibler's theory by considering fluctuations of the order parameter and redefined the structure factor by using a renormalized interaction parameter χ^{renorm} [21]. In this way, the disordered state of block copolymers was divided into two regimes: mean-field regime and fluctuation regime. For the present block copolymers, the Flory–Huggins parameter χ shows weak temperature variation. It is therefore difficult to discriminate both regimes in the experimentally accessible temperature range.

Another interesting observation is the fact that the solid state of a semicrystalline block copolymer may possess an equilibrium lamellar structure, resulting from the balance of extended-chain conformation favored by the crystalline block and the random coil conformation favored by the amorphous block [28]. This is quite different from the case of a semicrystalline homopolymer, in which the crystal thickness and chain-folded lamellar structure are metastable and kinetically controlled. Booth and coworkers [13–17] studied the solid state structure of low molecular weight EP, EPE, and PEP block copolymers, using SAXS and low-frequency Raman spectroscopy. It was shown that the PPO blocks in the PEP system reduced the melting point and increased the interface energy much stronger than in EP or EPE systems. While the chain-folded structures are more easily formed in PEP than in EP or EPE systems, the folding structure in EPE (Pluronics) systems is still in debate [8].

In this work, we consider the composition fluctuation and domain spacing of a series of commercially produced EPE block copolymers in the melt and in solid state. We mainly use SAXS to study the variation of structure with temperature and with time following temperature jumps. We show that mean-field behavior dominates in all samples in almost the whole temperature range in their melt state. A clear deviation from mean-field behavior was observed only on the relatively high M_w samples when approaching the crystallization of PEO block. In the solid state, the domain spacing increases with crystallization temperature. Depending on the length of PEO block and the crystallization temperatures, both chain-extended and once-folded structures are observed.

Experimental section

Materials

EPE triblock copolymers (Pluronics) were kindly supplied by BASF. To remove low molecular weight fractions, the copolymers were precipitated from dilute solution in benzene by addition of isooctane [14]. The precipitates were freeze-dried from benzene and then dried further in a vacuum oven at room temperature for 1 day. The basic parameters of the samples are listed in Table 1.

Table 1 Molecular characteristics of samples used in this work

Sample	Total molar mass	Molar mass PEO block	PEO block f (wt%)	T_c (°C) ^a	T_m (°C) ^a	ΔH_{fus} (J/g)
PE6400/E ₁₃ P ₃₀ E ₁₃	2,920	580	40	−30.4	20.3	10.0
PE6800/E ₈₀ P ₃₀ E ₈₀	8,750	3,000	80	18.3/22	51.0	114.6
PE9400/E ₂₁ P ₄₇ E ₂₁	4,600	920	40	1.45	36.42	66.6
PE10300/E ₁₇ P ₅₆ E ₁₇	4,750	750	30	−19.96	28.14	36.1
PE10400/E ₂₅ P ₅₆ E ₂₅	5,420	1,080	40	7.90	38.24	55.2
PE10500/E ₃₇ P ₅₆ E ₃₇	6,500	1,620	50	18.01	46.03	87.4

^aCrystallization (T_c) and melting (T_m) were obtained from standard DSC measurements, i.e., cooling and second heating scan with scanning rate of 10°C/min

Small-angle X-ray scattering

Two-dimensional SAXS was carried out with a Molecular Metrology System. The X-ray source is a sealed X-ray tube with copper anode. The wavelength of $Cu K_\alpha$ is $\lambda = 1.54$ Å. The X-ray beam is filtered by a Ni film of 10- μ m thickness and collimated by three pinholes. A 3.5-mm beam stop with an embedded photodiode is used for direct beam monitoring and sample transmission measurements. The scattered intensity is registered with an Ar-based multiwire 2-D detector (diameter of 200 mm), which is located 1.5 m from the sample. Thus, the accessible q -range is from 0.008 to 0.26 Å^{−1}. The intensity and photon efficiency of the detector were calibrated by the scattering of water. The angular scale was calibrated by the scattering peaks of silver behenate [29].

Samples in solid state or liquids with high viscosity were kept in a steel sample cell with mica windows. This cell was mounted in a holder with temperature controlled $\pm 0.1^\circ\text{C}$ in the range of -10 to 90°C by a Thermostat (HAAKE Phoenix II P1, Germany) with the coolant of glycerol and water. For each measurement in melt state, the samples were held at the preset temperature for 1,800 s. The measurement then takes another 3,600 s. In solid state, the samples were first isothermally crystallized in the sample holder for 1,800 s up to several hours (to be sure of complete crystallization). Then the measurement was taken at the crystallization temperature for 3,600 s. Background measurements were done with the empty sample holder at different temperatures, and no temperature dependence was observed. The total intensity and transmission of sample holder with or without sample was recorded for data treatment.

Data treatment The 2-D scattering pattern was calibrated by centering and was transformed to angular coordinates. Then it was converted to a 1-D scattering profile by azimuthal averaging of pattern. The intensity is presented in units of counts per pixel per second.

Background subtraction The raw data of sample and the background were divided by their experimental transmissions. The final intensity of sample was obtained by

subtracting the contribution of the background. Background from ambient radiation was ignored in all measurements due to its very weak contribution.

Time-resolved SAXS measurements

To study the effect of crystallization on the composition fluctuation in melt state, time-resolved measurements were carried out at temperatures in which crystal growth rate is low. Samples were first melted on a hot stage at 60°C for several minutes and then transferred to the sample holder, which was kept at the preset temperature T_c . The temperature jump to the preset T_c needs less than 240 s, and the measurements started 300 s later. Each measurement takes 200 s and the time interval between measurements is 5 s. Measurements for a given temperature were extended up to 7,200 s.

Results and discussion

Composition fluctuation in the liquid state

Figure 1 shows the SAXS profiles of a series of Pluronics during cooling. For the sake of clarity of presentation, only every tenth data point is shown. For samples with low PEO fraction (PE10300) or low molecular weight (PE6400, results not shown here), no concentration fluctuation could be observed (Fig. 1a). At high temperature or low value of the interaction parameter χN , the scattering intensity caused by concentration fluctuations is expected to be low. This is the case for the data shown in Fig. 1a. However, PE9400 (see Fig. 1b) shows a weak but detectable maximum, while PE10400 or PE10500 (Fig. 1c,d) display clear and strong scattering peaks. Upon cooling, the intensity increases with decreasing temperature. When the PEO blocks start to crystallize, the scattering intensity in the low q -range increases dramatically. For example, PE10400 at 30°C (Fig. 1c) presents a well-ordered crystalline lamellar structure with maxima at $q=0.024$ and 0.047 Å^{−1}, corresponding to the first and

second order of Bragg's peaks. At the same time, we see that the peak of composition fluctuation is still there.

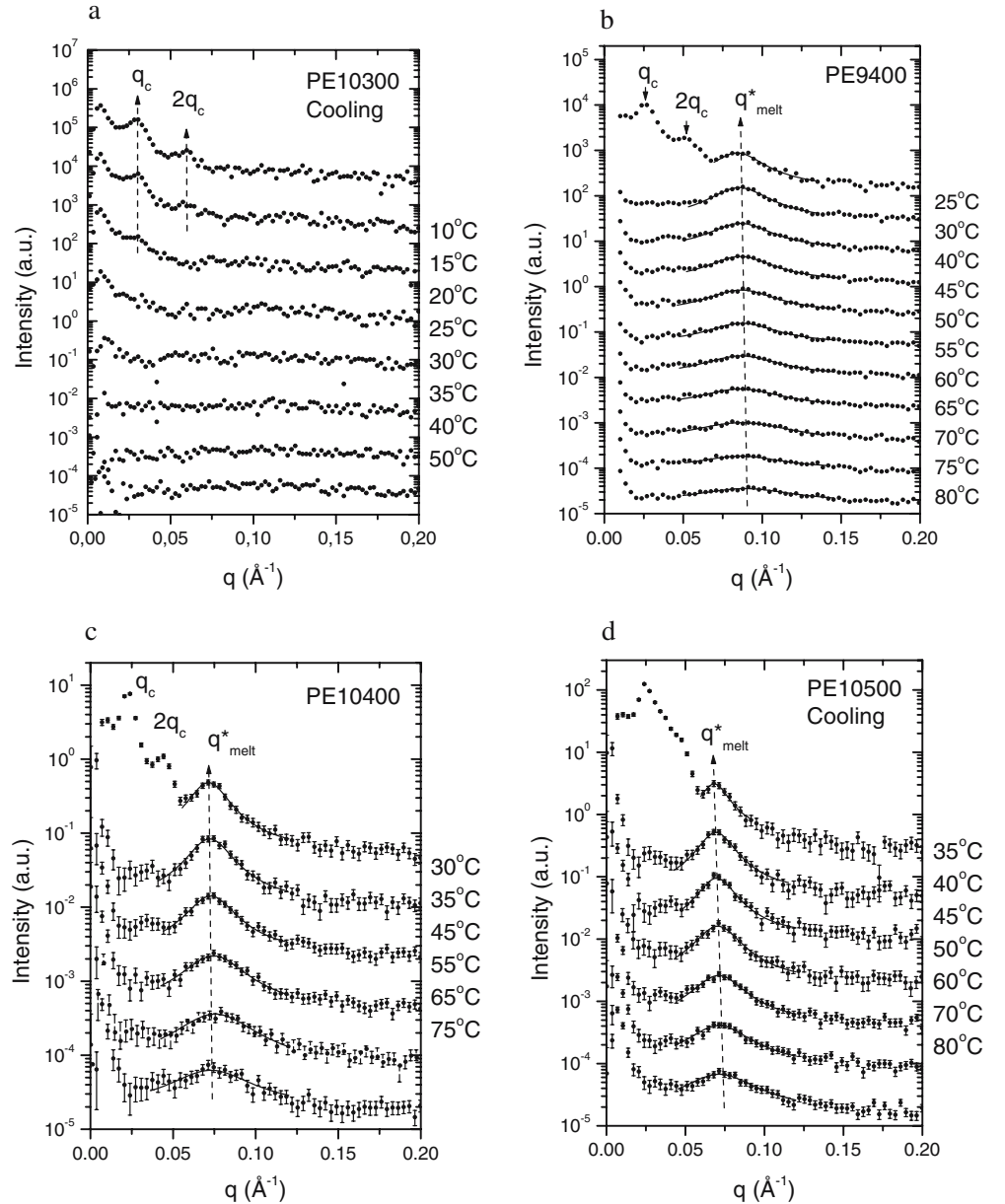
In view of the complexity of the scattering profile we analyze our data further using an approximate expression in place of Eq. 1. Expanding $F(q)$ around q^* to second order [22, 23] one arrives at an Ornstein–Zernicke type formula for the intensity caused by concentration fluctuations I_{cf} :

$$I_{cf} = y_0 + \frac{2A}{\pi} \frac{w}{w^2 + 4(q - q^*)^2} \quad (4)$$

$$\begin{aligned} \left(\frac{w}{2}\right)^2 &= \left(\frac{1}{\xi}\right)^2 \propto (1/R_g)^2 (\chi_s - \chi)/\chi_s \\ &\propto \frac{1}{N} (\chi_s - \chi)/\chi_s \propto 1/T_s - 1/T \end{aligned} \quad (5)$$

where w is the full width at half maximum of the intensity. This parameter is related to the inverse thermal correlation length (ξ) for composition fluctuations in the disordered state (Eq. 5). R_g is the radius of gyration of the block copolymer. With lowering temperature, ξ is expected to increase such that w^2 varies linearly with T^{-1} . The parameter y_0 in Eq. 4 takes background scattering into

Fig. 1 Temperature dependence of SAXS profiles of Pluronics during cooling. The intensities of the profiles shown at the bottom of each figure are actually measured values; the others were shifted up for clarity. **a** PE10300, **b** PE9400, **c** PE10400, and **d** PE10500. Only every tenth data point is plotted. The *solid lines* are fits according to Eq. 4



account, and q^* is the wave vector corresponding to the maximum intensity. Within mean-field theory, q^* should not vary with T . By fitting the SAXS profiles in Fig. 1, we thus obtain the values of the maximum intensity, I_{\max} , the peak position, q^* , and the full width at half maximum intensity, w . The corresponding period D_f was calculated as $D_f = 2\pi/q^*$. The temperature dependence of these parameters is displayed in Fig. 2.

Figure 2 shows D_f , w^2 , and I_{\max}^{-1} plotted as a function of T^{-1} for three samples. The values of w^2 and I_{\max}^{-1} decrease with T^{-1} , while D_f increases with T^{-1} . In all cases no discontinuous change could be observed. This is in accordance with observations made on block copolymers in their disordered state. It shows that the Pluronic copolymers do not exhibit microphase separation above their crystallization temperature as predicted previously [12]. However, we do see a clear deviation from the linear relationship at low temperature for the plots of D_f and I_{\max}^{-1} of sample PE10400 and PE10500. The increase of the period D_f is clearly seen in Fig. 2b. It indicates a stretching of the polymer coil as a consequence of concentration fluctuations. In the same temperature range, the inverse intensity I_{\max}^{-1} starts to deviate from its linear dependence. There exists a crossover from mean-field regime to fluctuation regime. From the plot of D_f and I_{\max}^{-1} , the crossover occurs between 40 and 45°C. On the other hand, the D_f values of PE9400 remain constant in the whole temperature range. This polymer obviously is in the mean-field regime.

From the variation of peak width and intensity with temperature, we can derive a measure for the distance of the system from the disorder to order transition. Both quantities, w^2 and I_{\max}^{-1} decrease with T^{-1} , and $I_{\max}^{-1} \sim T^{-1}$ display a linear relation at high temperature. Extrapolating I_{\max}^{-1} to zero we can obtain the spinodal phase separation temperature (T_s). The values found are 26.7, 18.7, and 4.0°C for PE10500, PE10400, and PE9400, respectively. However, the spinodal phase separation temperatures are not the true disorder to order phase transition temperature. With increasing concentration fluctuations, the system stabilizes its disordered state; therefore, the transition temperature is below T_s . For the polymers under study, we can conclude that there are no ordered phases in the melt state.

Time-resolved composition fluctuation during isothermal crystallization

Composition fluctuation is a typical feature of a block copolymer molecule in its disordered state. It reflects the overall conformation and size (radius of gyration) of the molecules, as well as the segmental interaction. The crystallization process, on the other hand, involves a conformation transition of molecules from a random

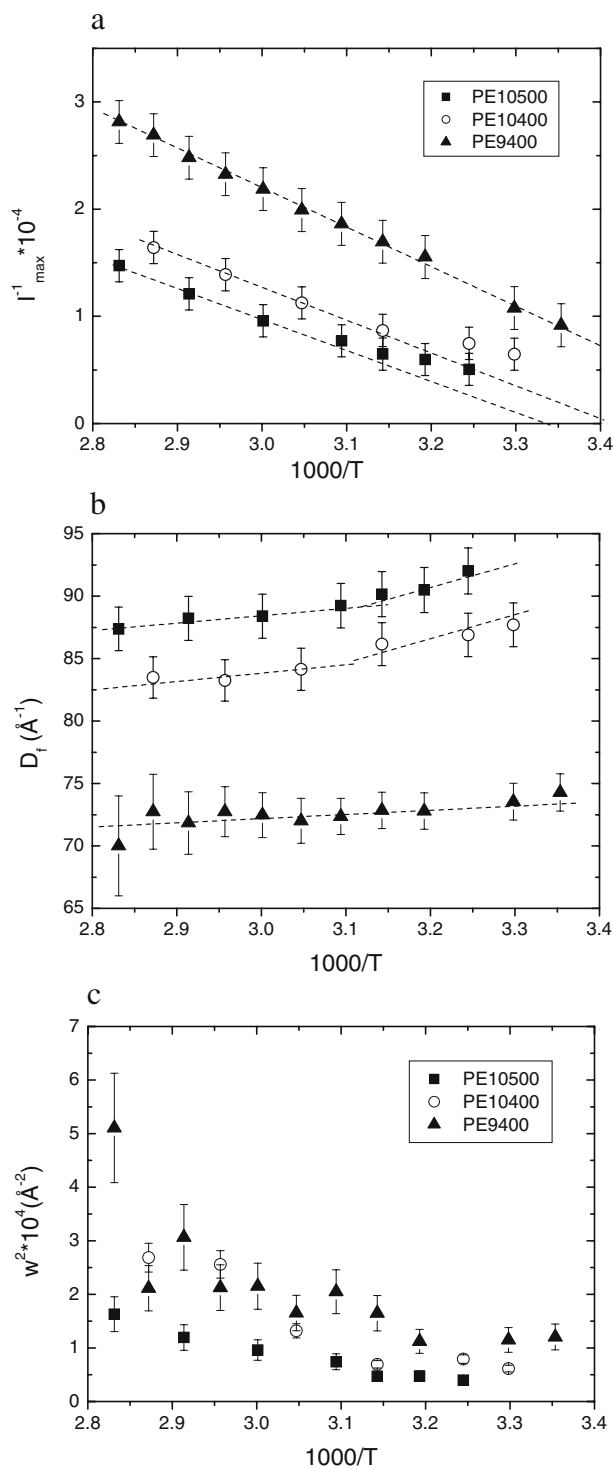


Fig. 2 Plots of I_{\max}^{-1} , w^2 and D_f vs T^{-1} . The data were obtained by fitting the SAXS profiles (Fig. 1) in the q range around the peak by Eq. 4

coil to a fully stretched conformation in the crystalline state. For the block copolymer molecules used in this work, the PEO blocks can crystallize, while the PPO

blocks are in their amorphous state. During the crystallization of the PEO blocks, not only do the PEO blocks change their conformation from random coil to stretched conformation, but also the PPO blocks due to the balance of the extended chain conformation favored by PEO block and the random coil conformation favored by PPO block. There is a long-standing problem in polymer crystallization, i.e., the existence of an intermediate state between disordered melt state and the final crystalline state [30]. In this study, by monitoring the composition fluctuation of disordered state, we may be able to shed light on this problem. In the following section, we study composition fluctuations during isothermal crystallization by using time-resolved SAXS.

Figure 3a shows an example of SAXS results of PE10500 during isothermal crystallization at 34°C. Each measurement takes 200 s and the interval time between each measurement is 5 s. Only every second profile is plotted in Fig. 3a for the sake of clarity. It is obvious that the scattering maximum due to concentration fluctuation appears in the inductive time of crystallization. It exists during the whole crystallization process, but it changes its shape and intensity step by step. The apparent I_{\max} increases constantly with time. To extract I_{\max} from the data, the contribution of scattering from the developing crystalline structure was taken into account by fitting the data with a combination of a linear background and a Lorentzian function (Eq. 6). In Fig. 3b, we present the result of this analysis as the time dependence of I_{\max} and q^* . The apparent I_{\max} read directly from the SAXS profiles is also presented in Fig. 3b.

$$I(q) = a - bq + \frac{2A}{\pi} \frac{w}{w^2 + 4(q - q^*)^2} \quad (6)$$

The apparent intensity increases constantly with time. After subtracting the contribution from crystallization, the I_{\max} remains constant until the early time of crystallization then it increases with time. The center of the peak q^* decreases with time without delay. These results indicate that the onset of crystallization of the PEO block enhances composition fluctuations of the remaining disordered state. Similar results were observed at different crystallization temperature (30–36°C not shown).

In further analysis on the solid state of this sample, we found that the scattering intensity attributed to concentration fluctuations may be influenced by a further contribution from the crystalline structure. Figure 4a shows a Lorentz-corrected SAXS profile of PE10500 crystallized at 34°C. From low to high q values, the first ($q = 0.064 \text{ \AA}^{-1}$) and the third peak ($q = 0.046 \text{ \AA}^{-1}$) corresponds to the first and second order of a lamellar structure, while the shoulder at $q = 0.032 \text{ \AA}^{-1}$ indicates the existence of a different lamellar structure. If this structure is sufficiently regular, its

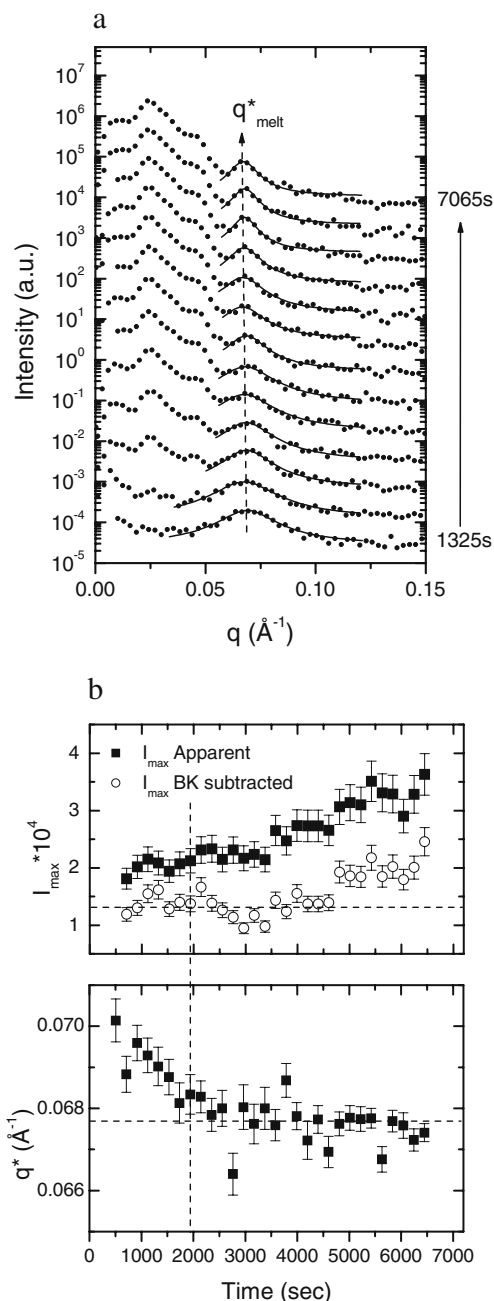


Fig. 3 **a** Time-resolved 1-D SAXS profiles of PE10500 crystallized at 34°C. Every second profile is shown. Only every tenth data point is plotted. The solid lines are fits of Eq. (6). **b** Plots of I_{\max}^{-1} , q^* of the peak of the composition fluctuation vs time. The vertical dashed line indicates the starting time of crystallization. It was determined from the first intensity profile in which the main intensity maximum of crystallization could be seen

second order reflection will be located at $q = 0.064 \text{ \AA}^{-1}$, slightly lower than the peak position of composition fluctuation. Therefore, this second order scattering might contribute to the scattering maximum (Fig. 3b). To remove this contribution, we used another sample (PE10400)

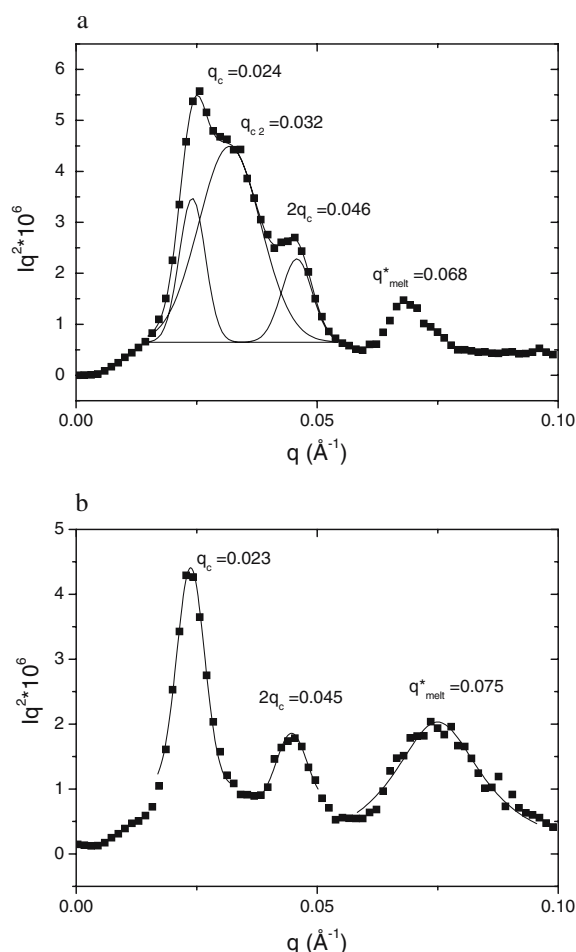


Fig. 4 Lorentz-corrected SAXS profiles for **a** PE10500, $T_c = 34^\circ\text{C}$ and **b** PE10400, $T_c = 33^\circ\text{C}$. Only every tenth data point is shown

crystallized at 33°C . Figure 4b presents the Lorentz corrected SAXS profile. It shows a very good lamellar structure with the two peaks corresponding to the first and second order. The third peak corresponds to the composition fluctuation. Even if there is a third order scattering of the crystalline structure, the intensity should be very weak and will not contribute significantly to the composition fluctuation. In this case, we can safely neglect the contribution from the crystallization. Figure 5 shows the time-resolved experimental results and the plots of I_{max} and q^* as a function of time. The apparent intensity does not change too much, but after subtracting the background, the intensity remains constant before crystallization and then decreases with time. At the same time, the q^* values slightly decreased.

The time resolved SAXS measurements provide information on the overall conformation of the remaining molecules in melt during crystallization. The variation of intensity with time is the result of the conversion of block copolymer molecules from the melt into the solid state with its crystalline/amorphous alternating lamellar structure.

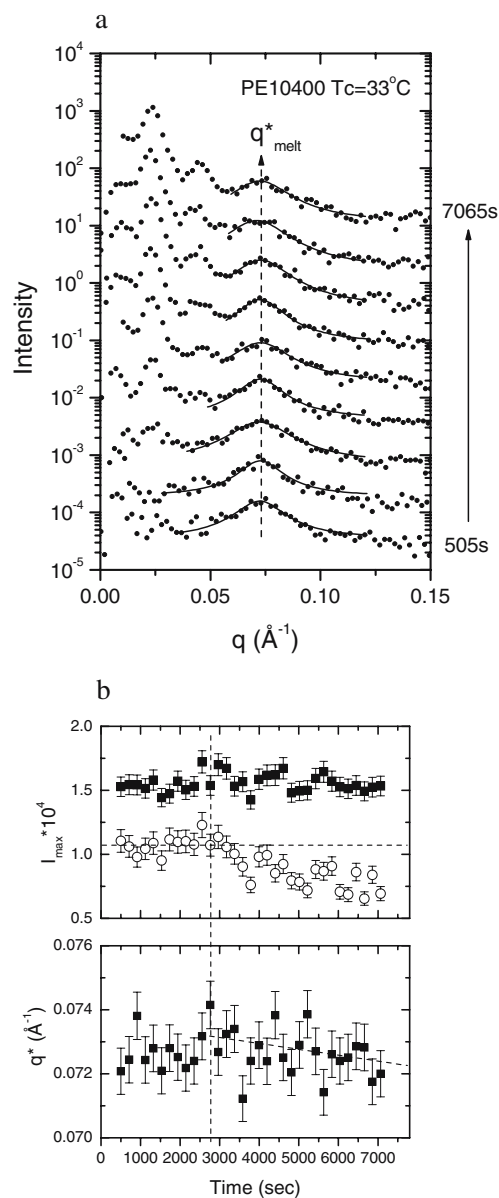


Fig. 5 **a** Time-resolved 1-D SAXS profiles of PE10400 crystallized at 33°C . Every fourth profile and only every tenth data point is shown. The solid lines are fits of Eq. 6. **b** Plots of I_{max}^{-1} , q^* of the peak of the composition fluctuation vs time. The vertical dashed line indicates the starting time of crystallization

The crystallization process reduces the amount of the copolymer molecules in the disordered state; therefore, it reduces the scattering intensity of composition fluctuation. This makes it difficult to recognize the effect of crystallization from the plot of I_{max} vs time. Figure 5 confirms this expectation.

An independent second observation is the position of q^* . Crystallization should not change the position of the peak. Furthermore, there may be a fractionation effect due to the polydispersity of the sample, i.e., the long PEO blocks

crystallize first, leaving the molecules with short PEO blocks in the disordered state. This effect will result in a shift of the intensity maximum to larger q . In all, there is no reason from crystallization to shift the peak position to a lower q value. However, in all of our experiments, we observe a decrease of q^* (Figs. 3b and 5b), albeit the decrease in Fig. 5b is small. Considering the fractionation effect, the observed decrease of q^* must result from the continuous stretching in the overall conformation of the molecules remaining in the disordered state.

Domain spacing in the solid state

Studies on the solid state of PEO/PPO copolymers showed that the polymers form well-ordered lamellar structures [8–10, 13–17]. The folding structure of PEO blocks depends on their length, the volume fraction, and the architecture of the polymer. In commercial products of the Pluronics type, phase separation in their melt state does not exist. The ordered solid state is induced by the crystallization of PEO blocks. We investigate the lamellar structure of the solid state formed at different crystallization temperatures.

Figure 6 shows typical 2-D SAXS patterns of PE6800 and PE10500 crystallized at lower and higher T_c , respectively. For the whole T_c range, PE6800 having 80% of PEO crystallize into spherulites with a size comparable with the size of the X-ray beam. Thus, the resulting pattern shows strong orientation (Fig. 6a,b). On the other hand, the SAXS patterns of other samples used in this work usually show an isotropic ring pattern, as shown in Fig. 6c,d. Detailed analysis on the solid structure was done by transferring the 2-D pattern into 1-D intensity profiles. The results are shown in Fig. 7 as plots of Iq^2 vs q . The domain spacing values are given in Table 2.

In Fig. 7a, the solid state of PE9400 shows two clear peaks in a large temperature range. The two peaks can be assigned as the first and second order scattering. Therefore, this sample forms a simple lamellar structure. The peaks of the first order shift toward a lower q value with increasing crystallization temperature. The intensity maximum of composition fluctuation observed in the melt state (Fig. 1b, $q \sim 0.78 \text{ \AA}^{-1}$) is absent in solid state. Similar SAXS profiles were observed for PE10400 in Fig. 7b. The first two peaks correspond to the Bragg scattering of a lamellar structure, and the intensity of the second order decreases with

Fig. 6 Typical 2-D SAXS patterns of **a** PE6800, $T_c=20^\circ\text{C}$; **b** PE6800, $T_c=45^\circ\text{C}$; **c** PE10500, $T_c=20^\circ\text{C}$; and **d** PE10500, $T_c=34^\circ\text{C}$

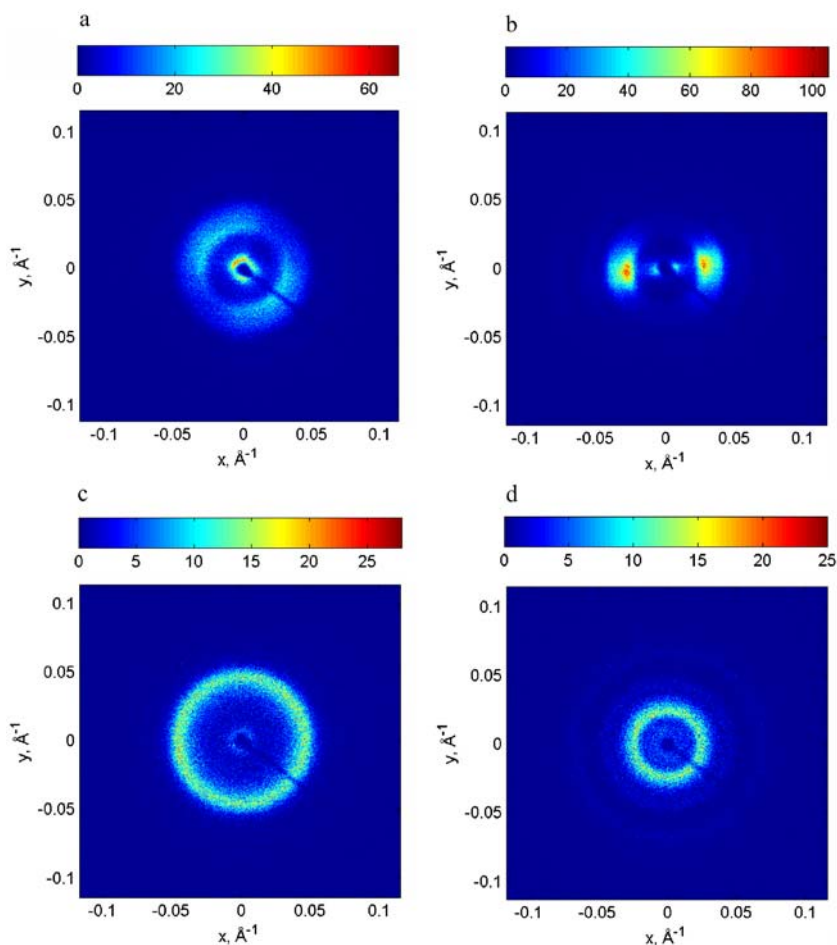
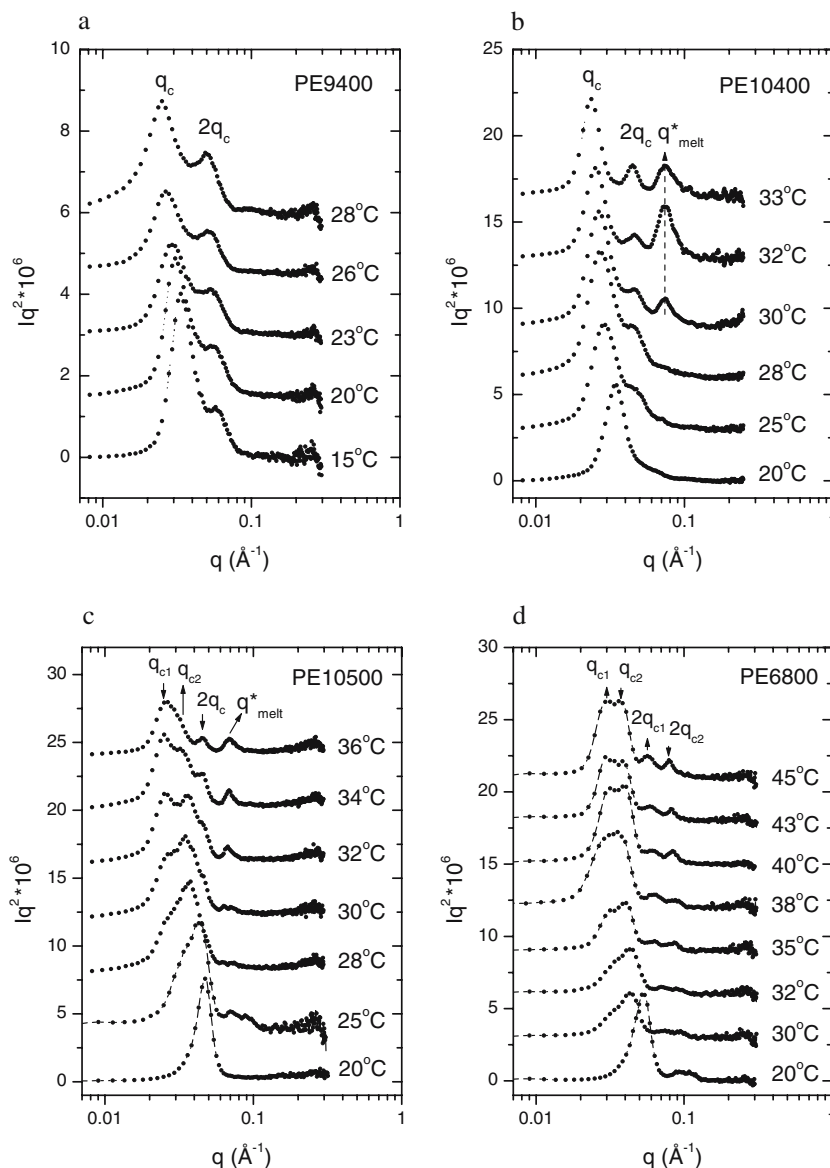


Fig. 7 Lorentz-corrected 1-D SAXS profiles of Pluronics crystallized at various temperatures. **a** PE9400, **b** PE10400, **c** PE10500, and **d** PE6800. Only every fifth data point is shown



decreasing temperature. At $T_c < 25^\circ\text{C}$, the second order peak disappears. Compared with Fig. 7a, there is a new peak shown at high q values in SAXS profiles of $T_c > 28^\circ\text{C}$. From the results of Fig. 1 and the time-resolved SAXS measurements (Figs. 3 and 5), it is clear that this new peak originates from the concentration fluctuation of the remaining molecules in the disordered state. This can be the result of the incomplete crystallization or fractionation effect.

The contributions from concentration fluctuation are also observed in PE10500 (Fig. 7c) at high crystallization temperatures ($T_c > 30^\circ\text{C}$). However, the scattering from the crystalline/amorphous structure in PE10500 is more complicated. In the SAXS profiles of $T_c > 28^\circ\text{C}$, the profiles can be fitted by three peaks with $q = 0.024$, 0.032 , and 0.047 \AA^{-1} , respectively (one example of $T_c = 34^\circ\text{C}$ is shown in Fig. 4a).

The positions of the peaks are almost constant with temperature, but their relative intensities change with T_c . From the positions of the peaks, the first and the third peaks can be assigned as the first and second order of a lamellar structure, while the second peak indicates the coexistence of another lamellar structure. The second order scattering of this lamellar structure either overlaps with the q^*_{melt} or is too weak to be observed. This coexistence in two-lamellar structures is reduced step by step to a simple lamellar structure at low crystallization temperatures ($T_c < 25^\circ\text{C}$).

The SAXS profiles of PE6800 in Fig. 7d show us a different situation. On one hand, due to the strongly asymmetric architecture, i.e., 80 wt% of PEO, the scattering maximum of composition fluctuation is not observed in the whole temperature range. On the other hand, the high

Table 2 Domain spacing of Pluronics in solid state

Sample	PE9400		PE10400		PE10500		PE6800	
Vol% PEO ^a	38.4		38.4		48.3		78.9	
$L_{\text{PEO}}/\text{\AA}^b$	59		70		103		223	
IF(0)/\AA	156		187		229		292	
IF(1)/\AA	78		94		115		146	
Domain spacing	$T_c/^\circ\text{C}$	$D/\text{\AA}$	$T_c/^\circ\text{C}$	$D/\text{\AA}$	$T_c/^\circ\text{C}$	$D/\text{\AA}$	$T_c/^\circ\text{C}$	$D/\text{\AA}$
	5	133	20	184	20	134	20	118
	10	148	25	220	23	146	30	143 / 188
	15	209	28	228	25	144 / 194	32	143 / 193
	20	191	30	240	28	173 / 247	35	144 / 193
	23	219	32	240	30	180 / 251	38	153 / 201
	26	238	33	266	32	175 / 252	40	153 / 203
	28	257			34	196 / 261	43	161 / 214
					36	209 / 257	45	166 / 230

^aThe volume fraction of PEO block in the melt state was calculated from the weight fraction (f wt%) in Table 1 by $\text{vol\%} = (f/\rho_{\text{PEO}})/(f/\rho_{\text{PEO}} + (1-f)/\rho_{\text{PPO}})$, where the density of amorphous PEO and PPO are $\rho_{\text{PEO}}=1.08 \text{ g/cm}^3$ and $\rho_{\text{PPO}}=1.01 \text{ g/cm}^3$, respectively [2]

^bThe length of PEO block in the crystalline state was calculated on the basis of a repeat distance of 19.5 \AA for seven units in the c direction of the PEO unit cell [13]

fraction of PEO results in a rich lamellar structure. For $T_c > 30^\circ\text{C}$, four peaks or shoulders may be discriminated. They correspond to the first and the second order of two lamellar structures. Similarly, this two-lamellar structure is also reduced to a simple lamellar structure at low temperature ($T_c < 30^\circ\text{C}$).

One question arising from earlier studies is whether the PEO blocks of Pluronics can form chain-folded structure in solid state. Svensson and Olsson [8] studied the phase behavior of two Pluronics ($\text{E}_{19}\text{P}_{43}\text{E}_{19}$ and $\text{E}_{13}\text{P}_{30}\text{E}_{13}$) with or without selective solvents, they found that with increasing temperature, the peaks move to lower q , while at the same time the overall scattered intensity decreases. They explained their observation that the domain spacing increases with temperature because not all PEO blocks are aggregated into the crystalline domains contributing to the lamellar structure. Hence, more PEO blocks are left in the amorphous domain with increasing temperature, thus leading to the increase of domain spacing and the decrease of scattering intensity. Domain spacing results from SAXS for four samples are given in Table 2. The domain spacing of extended chain [IF(0)] and once-folded [IF(1)] PEO block has been calculated based on the density model and is also listed in the table. For samples with short PEO block, such as PE9400 and PE10400, the long period values are close to or larger than their IF(0) structure in the whole T_c range. That means they are always in extended-chain crystalline state. This is consistent with the report of Svensson and Olsson [8]. On the other hand, by increasing the length of the PEO block, the SAXS results of PE10500

and PE6800 (Fig. 7c and d) show that the lamellar structures of IF(1) and IF(0) coexist in a large T_c range, and their relative fractions depend on crystallization temperature.

Conclusions

We have studied a series of PEO–PPO–PEO triblock copolymers (Pluronics) in their melt and solid states using SAXS. In the melt state, all samples are in a disordered state. Composition fluctuation could be observed for relative high molar mass sample with symmetric composition. The analysis of the temperature dependence of I_{max}^{-1} , w , and D indicated that the mean-field description was adequate in the whole temperature range, and the polymers may be considered to be in the weak segregation state. Deviations from this conformation could be observed when polymers start to crystallize. The composition fluctuation during crystallization was measured by time-resolved SAXS. The time dependence of I_{max} and q^* was analyzed. It was concluded that the overall conformation of the remaining molecules in the disordered state is stretched during crystallization.

In the solid state, crystallization of PEO induced phase separation results in a lamellar structure of alternating crystalline/amorphous layers. The folding structure and lamellar thickness strongly depend on the length of PEO blocks and crystallization temperatures. For Pluronics with short PEO blocks, the molecules in the crystalline states are

always in an extended-chain conformation, while for samples with $L_{\text{PEO}} > 100$ Å, once-folded structure was formed at low T_c .

Acknowledgement F. Zhang thanks the Alexander von Humboldt Foundation for awarding the Humboldt Research Fellowship.

References

1. Hamley IW (2000) The physics of block copolymer. Oxford Univ Press, New York
2. Mortensen K (2001) Polym Adv Technol 12:2
3. Alexandridis P (1997) Curr Opin Colloid Interface Sci 2:478
4. Wanka G, Hoffmann H, Ulbricht W (1990) Colloid Polym Sci 268:101
5. Yang J, Wegner G, Koningsveld R (1992) Colloid Polym Sci 270:1080
6. Luo YZ, Nicholas CV, Attwood D, Collett JH, Prince C, Booth C (1992) Colloid Polym Sci 270:1094
7. Wu G, Zhou Z, Chu B (1993) Macromolecules 26:2117
8. Svensson B, Olsson U (2000) Macromolecules 33:7413
9. Mortensen K, Brown W, Jørgensen E (1994) Macromolecules 27:5654
10. Mortensen K, Brown W, Jørgensen E (1995) Macromolecules 28:1458
11. Hamley IW, Castelletto V, Yang Z, Price C, Booth C (2001) Macromolecules 34:4079
12. Fairclough JPA, Yu GE, Mai SM, Crothers M, Mortensen K, Ryan AJ, Booth C (2000) Phys Chem Chem Phys 2:1503
13. Booth C, Pickles CJ (1973) J Polym Sci Polym Phys Ed 11:249
14. Booth C, Dodgson DV (1973) J Polym Sci Polym Phys Ed 11:265
15. Ashman PC, Booth C (1975) Polymer 16:889
16. Ashman PC, Booth C, Cooper DR, Price C (1975) Polymer 16:897
17. Viras F, Luo YZ, Viras K, Mobbs RH, King TA, Booth C (1988) Makromol Chem 189:459
18. Leibler L (1980) Macromolecules 13:1602–1617
19. Schwab M, Stühn B (1996) Phys Rev Lett 76:924
20. Bates FS, Rosedale JH, Fredrickson GH (1990) J Chem Phys 92:6255
21. Fredrickson GH, Helfand EJ (1987) Chem Phys 87:697
22. Sakamoto N, Hashimoto T (1995) Macromolecules 28:6825
23. Olvera de la Cruz M, Sanchez IC (1986) Macromolecules 19:2501
24. Stühn B, Mutter R, Albrecht T (1992) Europhys Lett 18(5):427
25. Schuler M, Stühn B (1993) Macromolecules 26:112
26. Mutter R, Stühn B (1995) Macromolecules 28:5022
27. Stühn B, Vilesov A, Zachmann HG (1994) Macromolecules 27:3560
28. Whitmore MD, Noolandi J (1988) Macromolecules 21:1482
29. Huang TC, Toraya H, Blanton TN, Wu Y (1993) J Appl Crystallogr 26:180
30. Strobl G (2000) Euro Phys J E Soft Matter 3:165